GEOCHEMISTRY

Correlation between tectonic CO_2 Earth degassing and seismicity is revealed by a 10-year record in the Apennines, Italy

G. Chiodini[1], C. Cardellini[1,2]*, F. Di Luccio[3], J. Selva[1], F. Frondini[2], S. Caliro[4], A. Rosiello[2], G. Beddini[2], G. Ventura[3,5]

Deep CO_2 emissions characterize many nonvolcanic, seismically active regions worldwide, and the involvement of deep CO_2 in the earthquake cycle is now generally recognized. However, no long-time records of such emissions have been published, and the temporal relations between earthquake occurrence and tectonic CO_2 release remain enigmatic. Here, we report a 10-year record (2009–2018) of tectonic CO_2 flux in the Apennines (Italy) during intense seismicity. The gas emission correlates with the evolution of the seismic sequences: Peaks in the deep CO_2 flux are observed in periods of high seismicity and decays as the energy and number of earthquakes decrease. We propose that the evolution of seismicity is modulated by the ascent of CO_2 accumulated in crustal reservoirs and originating from the melting of subducted carbonates. This large-scale, continuous process of CO_2 production favors the formation of overpressurized CO_2-rich reservoirs potentially able to trigger earthquakes at crustal depth.

INTRODUCTION

The relation between seismicity and fluid circulation has been demonstrated considering both the potential role of deep fluids in earthquake generation and the close spatial correlation between seismic zones and areas of deep fluid discharge (*1*, *2*). The role of deep fluids in earthquake triggering has been recognized in different tectonic settings, including compressional (*3*–*5*), strike-slip (*6*, *7*), and extensional (*8*–*12*) regimes. Besides, the involvement of CO_2-rich fluids in seismic sequences has been proven (*6*, *9*–*14*). A worldwide spatial correspondence between seismically active areas and CO_2 emissions has been demonstrated (*15*, *16*) as well as the primary role of extensional tectonics on Earth degassing of CO_2 (*2*). The few measured cases, Central-Southern Italy (*17*, *18*) and Eastern African rift (*19*, *20*), indicate the global relevance of tectonic CO_2 fluxes, which are thought to have controlled the CO_2 concentration of the atmosphere and thus of the climate (*21*).

The temporal variation of the rate of tectonic CO_2 discharge with seismicity is, however, still unconstrained because long time series of CO_2 discharge in seismically active areas have not been collected. Here, we show a 10-year-long (2009–2018) record of tectonic CO_2 emissions compared with seismicity in Central Apennine (Italy), an area where devastating historical earthquakes have occurred [e.g., the 1461 M_e (equivalent magnitude) 6.4 and 1703 M_e 6.7 events (*22*); http://storing.ingv.it/cfti/cfti5/]. The 2009–2018 observation period is a period of repeated seismic sequences (Fig. 1) that are considered here as a unique 10-year-long sequence (Central Apennine Seismic Sequence, hereinafter referred to as CASS). CASS includes the devastating main shocks of 6 April 2009 [M_w (moment magnitude) = 6.3, L'Aquila earthquake], 24 August 2016 (M_w = 6.0, Amatrice earthquake), and 30 October 2016 (M_w = 6.5, Norcia earthquake). These earthquakes and their stronger aftershocks destroyed over a large area of Central Italy with more than 600 deaths, 2000 injured, and evacuation of about 120,000 persons. The three major earthquakes occurred at similar depths (8 to 12 km) with thousands of aftershocks concentrated in the upper 10 to 12 km of the crust. These shocks were characterized by normal focal mechanisms with a northwest-southeast (NW-SE) rupture strike consistent with that of the major Apennine faults (*11*, *23*) that move in response to a northeast-southwest (NE-SW) extension. In the Apennine, crustal extension and devastating earthquakes occur in the overriding plate in response to regional uplift related to an uprising and eastward-moving mantle wedge (*17*, *24*–*27*). Our 2009–2018 degassing record of tectonic CO_2 flux shows that more than 1800 kt of deeply derived CO_2 were released from a relatively small area (~700 km^2) with a rate varying in time accordingly to the evolution of the seismicity.

RESULTS

Record of tectonic CO_2 emission compared with seismicity

Abundant, diffuse CO_2 degassing affects the western side of the Apennine chain (*17*) and confirms the occurrence of melting of subducting plate carbonates in the mantle (*25*). The upward migration of CO_2-rich fluids generates two large degassing structures at the surface: the Tuscan Roman degassing structure (TRDS) and Campanian degassing structure (CDS) that extend from the Tyrrhenian Sea to the Apennines (Fig. 1) (*17*). The seismic activity (http://terremoti.ingv.it/) mainly concentrates in the axial sector of the chain, at the eastern boundary of TRDS and CDS (Fig. 1). This intriguing spatial distribution, in light of the degassing structures, suggests that the gas, accumulated in buried highly pressurized structural traps, may favor seismicity (*17*, *27*), because high-pressure CO_2 at depths can promote fault weakening mechanism (*9*, *28*). CASS began at the eastern border of the TRDS (Fig. 1), where a deep source supplying endogenous carbon dioxide to the groundwater is detected.

The geochemical investigations aimed to detect and quantify the possible earthquake-related emission of deep CO_2 started immediately after the April 2009 mainshock (*29*); in particular, we focused

[1]Istituto Nazionale di Geofisica e Vulcanologia, Sezione di Bologna, via D. Creti 12, 40128 Bologna, Italy. [2]Dipartimento di Fisica e Geologia, Università degli Studi di Perugia, via Pascoli snc, 06123 Perugia, Italy. [3]Istituto Nazionale di Geofisica e Vulcanologia, Sezione di Sismologia e Tettonofisica, via di Vigna Murata 605, 00143 Rome, Italy. [4]Istituto Nazionale di Geofisica e Vulcanologia, Sezione di Napoli Osservatorio Vesuviano, via Diocleziano 328, 80124 Napoli, Italy. [5]Istituto per lo Studio degli Impatti Antropici e Sostenibilità in Ambiente Marino, CNR, via della Vasca Navale 79, 00146 Rome, Italy.
*Corresponding author. Email: carlo.cardellini@unipg.it

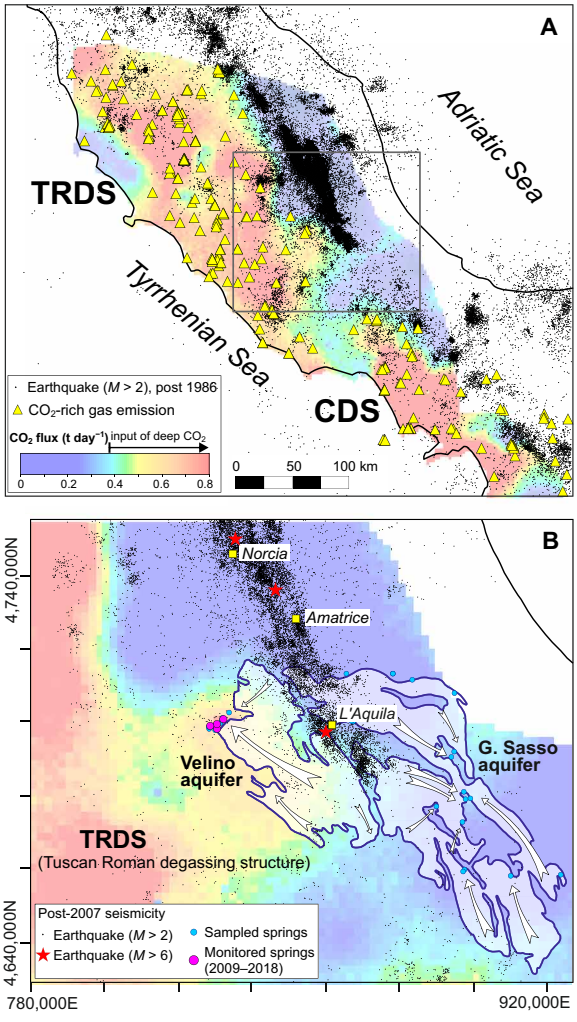

Fig. 1. Map of the seismicity and of CO_2 Earth degassing and location of investigated aquifers. (**A**) Map of the $M > 2$ 1986 to 2020 Italian seismicity recorded by the INGV (Istituto Nazionale di Geofisica e Vulcanologia) seismic network (terremoti.ingv.it; last accessed January 2020). (**B**) Studied aquifers and springs and the post-2007 seismicity. The main flow lines of the groundwaters are reported as arrows. Map of the CO_2 flux, modified from (*17*, *29*), is shown in the background of both (A) and (B). Coordinates are reported in UTM-WGS84-32N.

on the CO_2 dissolved in two large carbonate aquifers close to the epicentral areas (Gran Sasso and Velino aquifers; Fig. 1B). To date, the geochemical dataset includes 270 chemical and isotopic compositions of spring waters sampled from April 2009 to December 2018 (see Materials and Methods). These samples were collected at the main 36 springs (fig. S1) whose flow rate amounts to ~70% of the total discharge of the two aquifers (~80 $m^3\ s^{-1}$).

Concentration of deeply derived CO_2 (C_{deep}) is computed from the total dissolved inorganic carbon (TDIC) content of the water samples by applying a carbon mass balance (*30*) based on the carbon isotopes (see Materials and Methods). Remarkable variations are observed for three springs of Velino aquifer that were monitored for the entire period (Peschiera, Canetra, and San Vittorino), while the five springs of the Gran Sasso aquifer, monitored until 2015, show either a weak signal or no substantial variation in C_{deep} when compared to the Velino springs (fig. S2). C_{deep} of these latter springs follows the temporal evolution of the seismicity (Fig. 2, A to C). Peak values of C_{deep} occur concurrently with the main shocks [i.e., the devastating events of M_w 6.3 April 2009 and M_w 6 and M_w 6.5 August to October 2016; Fig. 2], and then CO_2 emissions decrease following the seismicity decay in terms of magnitude and rate. The robustness of the correlation between CO_2 and seismicity was investigated by testing the null hypothesis of no correlation (Pearson's correlation coefficient equal to 0) through the Student's t distribution (*31*). The C_{deep} is compared with the earthquake number, and the seismic energy release occurred at variable distance from the springs in a period centered at the sampling date ± a time lag. The correlation is statistically significant (significance level, 0.01) for a wide range of values for time lag (>10 days) and distance (20 to 80 km) (see Materials and Methods and fig. S3). This correlation is also well highlighted in the binary plots of Fig. 2 (A to C), where the C_{deep} content of the three springs is compared with the number of earthquakes for a time lag of 40 days, at a distance <45 km. It is worth noting the high correlations of the earthquake number with the C_{deep} of San Vittorino spring (the water that showed the strongest variation, $R^2 = 0.80$) and Peschiera spring (the spring of highest flow rate, $R^2 = 0.62$).

Although geochemical anomalies in groundwaters associated with CASS were already reported in many studies [e.g., (*32*–*34*) and references therein], we produce an unprecedented record of tectonic CO_2 emission (Fig. 2E) by applying a carbon mass balance to the Velino aquifer springs of known flow rate (see Materials and Methods). The daily flux of deeply derived CO_2 (F_{CO2}), similarly to C_{deep} of the springs, shows a statistically significant correlation with seismicity (significance level, 0.01; see Materials and Methods and fig. S3). The total cumulative amount of the CO_2 released during the CASS period (10 years) is of ~1800 kt, i.e., of the same order of magnitude of the CO_2 involved in volcanic eruptions [see Table 2 in (*35*)]. It is worth noting that this amount is the minimum estimate of the total CO_2 involved, because it does not include neither the degassed fraction of CO_2 (i.e., part of the CO_2 is directly emitted in the atmosphere by gas emissions; see movie S1) nor the gas emitted in other areas.

Origin of the CO_2

Decarbonation triggered by frictional heating in the slip zone of carbonate-hosted faults has been suggested as a possible CO_2 release mechanism during earthquakes [e.g., (*36*, *37*)]. However, this is not the case for CO_2 at the Velino aquifer, because the thermometamorphic CO_2 would have a very positive carbon isotope signature, as computable by theoretical fractionation and measured in laboratory experiments [$\delta^{13}C > +3$ per mil (‰); (*36*)]. Instead, the Velino waters show the input of CO_2 with a slightly negative carbon isotope signature ($\delta^{13}C \sim -1.5$‰) during the entire observation period (Fig. 3), therefore excluding a major contribution of CO_2 formed by frictional heating during the earthquakes.

The gas source must be sought in the westward subduction of carbonates of the Adriatic plate beneath the Tyrrhenian mantle. According to (*25*), melting of such carbonates, due to the high temperatures at the interface between the mantle wedge and the subducting plate, generates carbonate-rich melts. These low density and viscosity melts can migrate upward through the mantle causing zones of partial melting (and CO_2-rich compositions) whose presence at depths from 130 to 60 km is revealed by shear-wave velocity images (*25*). The lower pressures at shallower depths (<60 km) may induce massive CO_2 degassing and accumulation beneath the Moho

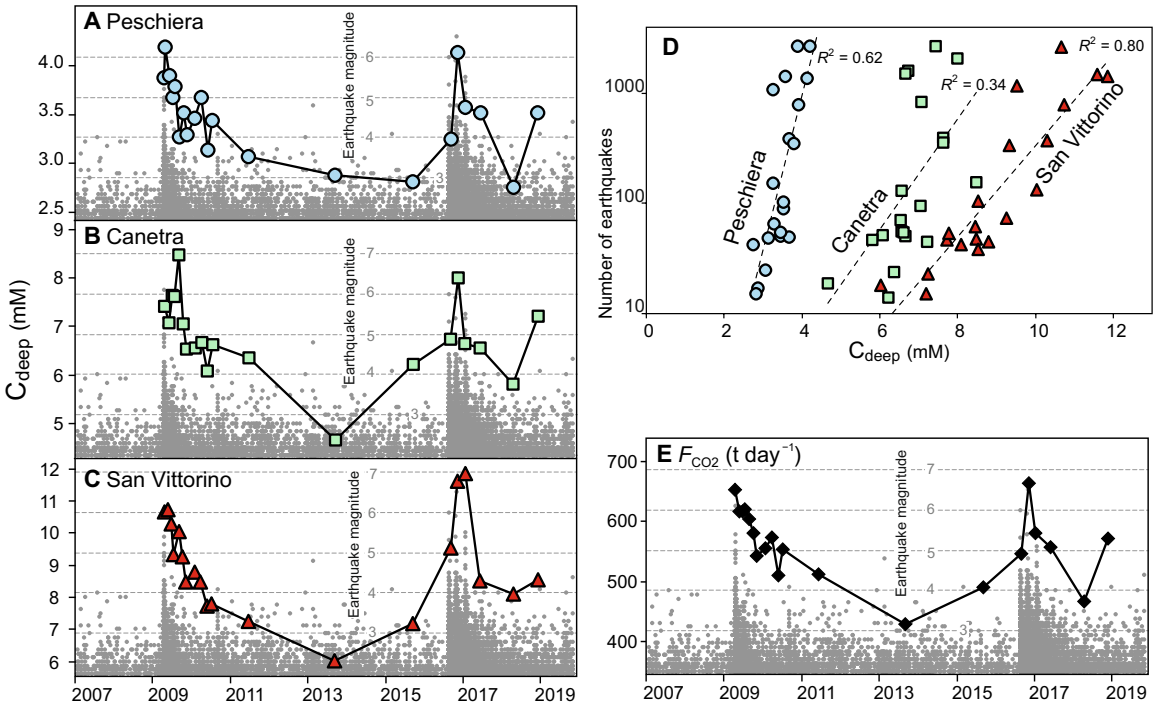

Fig. 2. Temporal evolution of CO_2 degassing and seismicity. (**A** to **C**) Chronograms of the earthquake magnitudes compared with the concentration of deeply derived carbon (C_{deep}) in the monitored springs. (**D**) Binary plots of C_{deep} of the monitored springs against the log number of the earthquakes occurred at distances <45 km in a period of 80 days centered at any sampling date. (**E**) Chronogram of the earthquake magnitudes compared with the daily amount of deeply derived CO_2 dissolved by the groundwaters of the Velino aquifer (F_{CO2}).

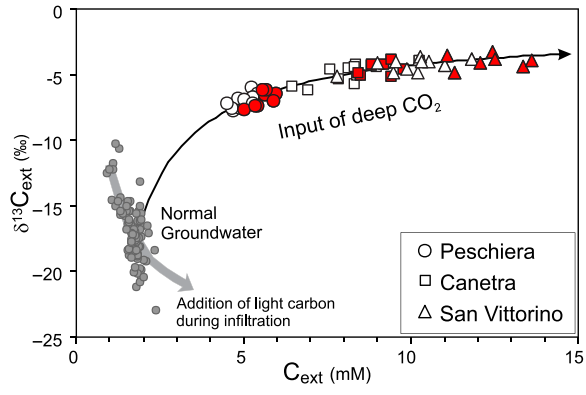

Fig. 3. CO_2 sources and dissolved carbon in the monitored springs. $\delta^{13}C_{ext}$ versus C_{ext} diagram of the monitored springs from the Velino aquifer. Measurements are compared with the theoretical compositions obtained adding a deep inorganic CO_2 ($\delta^{13}C = -1.48‰$) to normal groundwaters. Samples taken in periods close to the main earthquakes (red symbols) show evident shifts toward the same deep CO_2 component (i.e., of similar isotopic carbon signature) that enter the aquifer during the quiescence periods (white symbols).

and within the lower crust (*25*). The presence of a crustal CO_2 reservoir at 10- to 15-km depth in the L'Aquila basin, where the CASS started in 2009, is indicated by a sill-like negative anomaly of P-wave seismic velocity (V_p) (Fig. 4) and low ratio of P and S-wave seismic velocities (V_p/V_s) zone [see Fig. 4 in (*38*)]. This zone was interpreted as a CO_2 storage zone (*39*) fed by fluids from the underlying mantle wedge. The feeding process explains the high geothermal advective heat fluxes (~200 to 300 mW m^{-2}) transmitted through the aquifers located in the area (*39*). The deep CO_2 storage zone is underneath a great portion of the Velino aquifer (Fig. 4), where CO_2 emission has been documented. It is worth noting that the total thermal energy associated with the CO_2 emission during 2009–2018 is two orders of magnitude larger than the total seismic energy released by CASS (~6×10^{23} versus ~6×10^{21} erg; see Materials and Methods).

The deep origin of the tectonic CO_2 detected at Velino aquifer is also in agreement with previous seismological studies that highlighted the primary role of deep fluids in triggering and controlling the temporal evolution of CASS and of previous seismic sequences (*10*, *11*, *40*, *41*). For example, gas pulses from deep, highly pressurized reservoirs are recognized as the main source of the 1997 Umbria-Marche aftershocks (*9*) and of the 2013 Sannio-Matese earthquakes, these latter related to gas release from a magma intrusion in the lower crust (*12*).

DISCUSSION

In the Apennine chain, the crustal CO_2 reservoirs such as that located below the Velino aquifer (Fig. 4) are fed by the ascent of CO_2-enriched slab-derived fluids (*25*), a process implying a continuous mechanism of CO_2 production and accumulation in the crust. This ceaseless movement of CO_2 from depth causes pressurization in the reservoir and consequent transfer of gas to the uppermost crustal layers and, ultimately, CO_2 saturation-oversaturation of the overlying aquifer(s). At regional scale, this mechanism explains the formation of the large CO_2 degassing structures (TRDS and CDS in Fig. 1) and the formation of numerous emissions of free gas (Fig. 1).

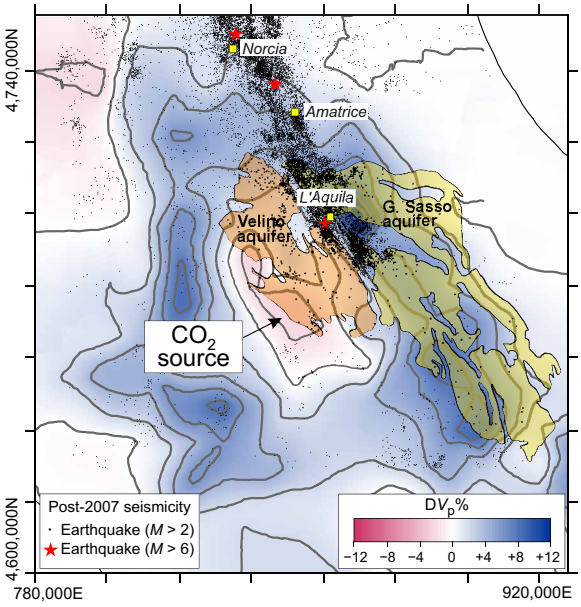

Fig. 4. V_P anomalies and source of the CO_2. The image highlights a negative anomaly in the seismic velocity variations (DV_p %) at 16-km depth [*P*-wave model (*38*)]. We interpret this anomaly as a deep gas storage zone that provides deeply derived CO_2 to the above located Velino aquifer. The top of the low V_P zone is located at a depth of 10 to 15 km [see Fig. 7 in (*39*)]. Coordinates are reported in UTM-WGS84-32N.

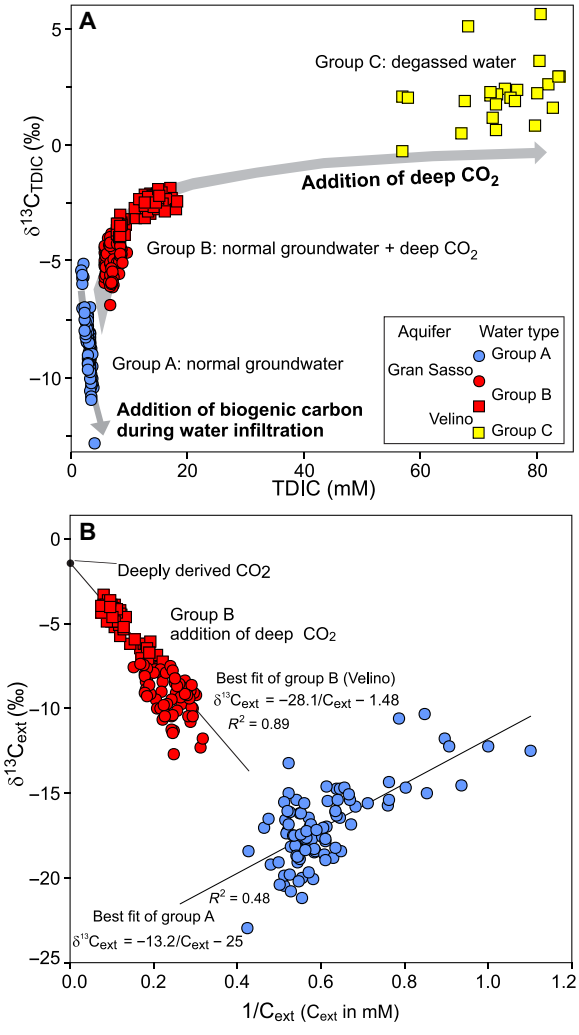

Fig. 5. Carbon dissolved in Velino and Gran Sasso groundwaters. (**A**) TDIC versus $\delta^{13}C_{TDIC}$ diagrams of the sampled water. Group A groundwaters (normal groundwaters) follow a trend expected for an infiltrating water dissolving an isotopically "light" biogenic CO_2. Group B and C groundwaters follow a trend compatible with the input of inorganic CO_2, characterized by a heavier $\delta^{13}C$ value. The high TDIC and the $\delta^{13}C$ values of group C suggest that these groundwaters are affected by CO_2 degassing before the sampling. (**B**) $1/C_{ext}$ versus $\delta^{13}C_{cext}$ diagram. The diagram allows the estimation of the isotopic composition of the deeply derived CO_2 and the infiltrating water end members.

The occurrence of CO_2 saturated-oversaturated waters at the Velino basin is testified by the Terme di Cotilia springs, which discharge hundreds of liters per seconds of CO_2 oversaturated waters, and by the direct emissions of a CO_2-rich gas phase (movie S1). Different mechanisms have been proposed for the transfer of CO_2-rich fluids from depth to surface. These include the dynamic, long-term fluid pumping of fluids related to grain-size reduction through the nucleation phase in the ductile mantle-crust shear zone (*42*), the ascent of fluids along deep-seated faults (*43*), the fluid pressurization by self-sealing processes and release (fault-valve) during earthquakes at the base of the seismogenic layer of the crust (*44*), and the emplacement of magma within the crust (*12*). Here, we propose that, in addition to the above processes, seismic shaking causes sudden ascent of already separated gas bubbles and, possibly, new gas exsolution from the CO_2-rich solutions (mechanical bubbling such as a shaken bottle of a carbonated drink). This process of fluid release is consistent with (i) the observed, almost simultaneous, increase of deep CO_2 with earthquakes at the surface (Fig. 2) and (ii) the occurrence at depth of earthquakes triggered by a fluid-related pressure front as suggested by the diffusive spatiotemporal evolution of the earthquakes (*11*). The increase of tectonic CO_2 flux at the surface can be caused by the gas released at shallow depths, while the formation of fluid-related pressure fronts would be explained by the gas separated at depth and by the ascent of increasing amounts of CO_2 from the deep reservoir. It is worth noting that this process implies a feedback because seismicity causes gas separation with the formation of ascending pressurized gas fronts that, in turn, favor seismicity.

The ascent of fluids in tectonically active zones may be a passive process favored by fracturing of the crust during earthquakes and/or an active process in which pressurized fluids rise to the surface along preexisting faults, thus triggering earthquakes. Taking into account (i) the close relationship between CO_2 discharge and rate/magnitude of the 2009–2019 CASS earthquakes (Fig. 2), (ii) the diffusive processes of seismicity migration and rate (*11*), (iii) V_P and V_P/V_s tomographic models (*45*), (iv) variations in fluid pore pressure during the preparatory phase of the 2009 and 2016 mainshocks (*46*), and (v) the fluid pressure larger than the regional minimum horizontal stress in the upper crust during the Apennine seismic sequences (*10*, *11*), we propose that the influx of CO_2 modulates the evolution of CASS.

We conclude that the ascent of huge amount of slab-derived CO_2 that continually accumulates at depth may significantly contribute to earthquake occurrence in the Apennines and, potentially, to the observed uplift (*47*) of the chain. The analysis of long-term time series of CO_2 discharge as presented here should be extended to other seismically active areas to better constrain the role of fluids

in modulating the seismic activity and to estimate the overall tectonic CO_2 flux on Earth.

MATERIALS AND METHODS

Field and laboratory measurements of groundwater

The complete dataset of the waters used in this work is reported in data file S1, while their location is reported in fig. S1. The first survey was performed in 1997, while the other surveys were carried out after the 2009 L'Aquila earthquake. Overall, 36 springs were sampled. Among these, 14 springs were monitored from 2009 to 2015: 4 springs belong to the Velino carbonate aquifer (total discharge Q_{tot} = 30.0 $m^3 s^{-1}$; sampled discharge Q_s = 24.75 $m^3 s^{-1}$), and 10 springs belong to the Gran Sasso carbonate aquifer (Q_{tot} = 49 $m^3 s^{-1}$; Q_s = 25.6 $m^3 s^{-1}$). The Velino aquifer springs, which showed remarkable variations, were sampled other six times after the earthquake of August 2016. Data collected in 1997 and from April 2009 to February 2010 were previously published (*29*, *30*) (see data file S1).

For each spring, temperature, pH, Eh, electrical conductivity, and total alkalinity were determined directly in the field. The alkalinity determination was performed by acid titration with 0.01 N HCl. Water samples for chemical analyses were filtered with 0.45-μm filters and collected in three 100-ml polyethylene bottles. One aliquot was immediately acidified with HCl 1:1 diluted.

For the determination of $\delta^{13}C$ of TDIC ($\delta^{13}C_{TDIC}$), the dissolved carbon species were precipitated in the field as $SrCO_3$ by adding $SrCl_2$ and NaOH in solid state to the water sample. Carbonate precipitates were then filtered and washed with distilled water in a CO_2-free atmosphere in the laboratory.

Dissolved ions were analyzed at the laboratory of Earth Science Department of Perugia University. Dissolved anions (Cl, F, SO_4, and NO_3) were determined by ion chromatography using a Dionex DX-120, Ca and Mg were determined by atomic absorption flame spectroscopy on the acidified sample, while Na and K were determined by atomic emission flame spectroscopy. All the laboratory analytical methods have an accuracy better than 2%.

Analyses of water hydrogen and oxygen stable isotopes (δD and $\delta^{18}O$) and of $\delta^{13}C_{TDIC}$ were performed at INGV (Istituto Nazionale di Geofisica e Vulcanologia, Sezione di Napoli), using a Finnigan Delta plus XP continuous flow mass spectrometer coupled with a GasBench II device. Each sample was analyzed in replicate. Carbon samples were analyzed versus the Working Standard Marmo Acqua Bianca (MAB) (marble, $\delta^{13}C$ = 2.45‰ and $\delta^{18}O$ = −2.43‰ versus Vienna Pee Dee Belemnite, V-PDB) (analytical errors: 1σ < 0.06‰). Oxygen and hydrogen isotope were analyzed versus five Working Standard [standardized versus Vienna Standard Mean Ocean Water (V-SMOW), Greenland Ice Sheet Precipitation (GSIP) and Standard Light Antarctic Precipitation (SLAP), International Atomic Energy Agency (IAEA) standards] using equilibration techniques (analytical errors: 1σ < 0.08‰ and <1.0‰ for oxygen and hydrogen, respectively). The TDIC and CO_2 partial pressure (P_{CO2}) were computed using the code PHREEQC (*48*) starting from the field determinations of T, pH, and alkalinity and the major ion concentrations.

Classification of the groundwaters

All samples show δD and $\delta^{18}O$ values typical of local meteoric waters and a Ca(Mg)-HCO_3 chemical composition (data file S1). The samples are classified into three groups (groups A, B, and C; Fig. 5A) based on their different TDIC and $\delta^{13}C_{TDIC}$. According to (*30*), the TDIC of the groundwater of carbonate aquifers is given by the sum of the carbon from dissolution of the carbonate minerals (C_{carb}) and the carbon from sources external to the aquifers (C_{ext}). The different origin of C_{ext} allows us to differentiate the normal groundwaters (low TDIC, group A) from group B and C samples (higher TDIC). In detail, C_{ext} is given only by the dissolution of biogenic carbon during the infiltration of the recharging water in group A (C_{inf}, the carbon concentration of the infiltrating water), whereas C_{ext} also originates from the addition of deeply derived CO_2 (C_{deep}) to normal groundwater in groups B and C (Fig. 5). The group C waters can be differentiated from group B given its higher amounts of added C_{deep} that causes CO_2 degassing (P_{CO2} ~1 bar in group C waters), calcite precipitation, and isotopic fractionation during the carbon removal.

Carbon mass balance

To quantify the contribution of the different carbon sources and to characterize their isotopic composition, we compute for each sample C_{ext} and $\delta^{13}C_{ext}$ using the following carbon mass balance equations

$$C_{ext} + C_{carb} = TDIC \quad (1)$$

$$\delta^{13}C_{ext} \times C_{ext} + \delta^{13}C_{carb} \times C_{carb} = \delta^{13}C_{TDIC} \times TDIC \quad (2)$$

where (i) TDIC and $\delta^{13}C_{TDIC}$ are analytically determined; (ii) C_{carb} is computed as the sum of Ca + Mg − SO_4 considering the dissolution of carbonate minerals (i.e., calcite and dolomite) and the possible presence of gypsum/anhydrite; and (iii) $\delta^{13}C_{carb}$ is assumed to be constant and equal to the average $\delta^{13}C$ of numerous samples of carbonate rocks from the investigated aquifers [+1.8‰; (*29*) and references therein].

The two equations can be used to determine C_{ext} and $\delta^{13}C_{ext}$ only for waters that have not experienced CO_2 degassing and calcite precipitation, a condition that, for the studied aquifers, is verified for TDIC <40 mM (*29*), i.e., only for the samples of group A and group B (Fig. 5A).

The concentrations (C_{inf} and C_{deep}) and isotopic compositions ($\delta^{13}C_{inf}$ and $\delta^{13}C_{deep}$) of the carbon from the different sources contributing to C_{ext} of group B samples are computed by considering the following carbon balance

$$C_{inf} + C_{deep} = C_{ext} \quad (3)$$

$$\delta^{13}C_{inf} \times C_{inf} + \delta^{13}C_{deep} \times C_{deep} = \delta^{13}C_{ext} \times C_{ext} \quad (4)$$

The system of two equations and four unknown variables is solved for each sample using the binary plot $\delta^{13}C_{ext}$ versus $1/C_{ext}$ (Fig. 5B) where mixtures among different sources show a linear trend. In particular, in the case of the springs of Velino aquifer:

(i) The isotopic compositions of the deeply derived CO_2 ($\delta^{13}C_{deep}$ = −1.48‰) is considered unique and derived in Fig. 5B as the $\delta^{13}C_{ext}$ intercept at $1/C_{ext}$ = 0 (i.e., pure CO_2 end member) of the best-fit linear regression ($\delta^{13}C_{ext} = -1.48 - 28.1/C_{ext}$) of the samples;

(ii) C_{inf} is determined at the interception of the line connecting each sample to the deep source ($1/C_{ext}$ = 0, $\delta^{13}C_{ext}$ = −1.48‰) with the infiltrating water line ($\delta^{13}C_{ext} = -25.0 + 13.2/C_{ext}$) computed as the best-fit linear regression of group A (normal groundwater). This sample by sample computations gives a narrow range of C_{inf} values, from 1.5 to 2.18 mM with a mean C_{inf} = 1.76 ± 0.18 mM;

(iii) the carbon concentration of the deeply derived CO_2 (C_{deep}) of each sample (Fig. 2, A to C) is given by inserting the computed mean C_{inf} in Eq. 3.

Note that, to have a minimum estimate of the C_{deep}, a simplified computation is applied also to the group C Terme di Cotilia spring, where part of the carbon is removed during degassing and calcite precipitation. In details, we compute C_{ext} from Eq. 1 and C_{deep} from Eq. 3, assuming the mean C_{inf} value derived for the group B waters.

Total CO_2 and energy output from Velino aquifer

The total deeply derived CO_2 entering the Velino (F_{CO2}) is computed by summing the contributions of the monitored springs and applying a correction to account for the portion of the nonsampled groundwaters. The different contributions are computed by multiplying the C_{deep} of the four monitored springs for a corresponding water discharge. For this computation, we consider the Peschiera, Canetra, Terme di Cotilia, and San Vittorino springs as representative of the discharge from groups of springs of similar compositions sampled in the detailed survey of January–February 2010. We consider a flow rate of 18 $m^3 s^{-1}$ for Peschiera, 6 $m^3 s^{-1}$ for the Canetra group, 0.25 $m^3 s^{-1}$ for Terme di Cotilia, and 0.5 $m^3 s^{-1}$ for the San Vittorino group according to data from detailed hydrogeological studies (*49*, *50*). Last, we scale the computed total CO_2 of the monitored springs (24.75 $m^3 s^{-1}$) to the total discharge of the aquifer (i.e., 30 $m^3 s^{-1}$).

The total energy associate with the deep CO_2 influx in the Velino aquifer is estimated starting from the good correlation between the deep CO_2 and the advective geothermal heat computed by (*39*) and (*18*) for 11 aquifers of the Central Apennine [which includes also the Velino aquifer, named Marsica N in (*39*)]. The good correlation suggests that the gas and the heat are advectively transported into the aquifers by hot CO_2-rich fluids. The estimated CO_2 flux from the data of each survey was used to estimate the thermal energy by applying the relation between the F_{CO2} (in t day^{-1}) and the geothermal heat flow (Q_H in erg day^{-1}), $Q_H = 3.3 \times 10^{17} F_{CO2}$, computed by the data reported in (*18*).

Correlation between deep CO_2 and seismicity

To track the deep CO_2, we consider four time series: C_{deep} from Peschiera, Canetra, and San Vittorino springs and F_{CO2}. The earthquake catalog includes seismic events with M_w >2.0 from September 2007 to August 2019. We verified the completeness of the catalog for this period and magnitude range. For each C_{deep} value, we extract from the catalog earthquakes within a given time lag before and after the sampling date and within a given distance from the corresponding spring (from Peschiera spring in the case of F_{CO2}), evaluating the number and the energy release (*51*) of the extracted events. In this way, for each C_{deep} and F_{CO2} time series and each couple time lag–distance, we build two seismic time series considering the logarithm of the earthquake number and of the total energy release.

We test the correlation between each C_{deep}-F_{CO2} series and each corresponding seismic time series (log number and energy) for a wide range of time lags (from 7 to 70 days) and distance (from 15 to 100 km). In each case, we test the null hypothesis of no correlation (Pearson's correlation coefficient equal to 0) through the Student's *t* distribution (*31*). As shown in fig. S3, the null hypothesis of no correlation can be rejected at significance levels of 0.05 and 0.01 for all time lags (>15 days) and distances (>30 km), with the exception of the case of C_{deep} at Canetra. In this specific case, the null hypothesis can be rejected at this significance level of 0.01 only for a limited set of time lags and distances for the log seismic energy and cannot be rejected for the number of earthquakes. Also considering the multiple tests performed, the overall correlation between deep CO_2 and the seismicity can be considered statistically significant.

SUPPLEMENTARY MATERIALS

Supplementary material for this article is available at http://advances.sciencemag.org/cgi/content/full/6/35/eabc2938/DC1

REFERENCES AND NOTES

1. S. A. Miller, in *Advances in Geophysics*, R. Dmowska, Ed. (Elsevier, Amsterdam, 2013), vol. 54, pp. 1–46.
2. G. Tamburello, S. Pondrelli, G. Chiodini, D. Rouwet, Global-scale control of extensional tectonics on CO_2 earth degassing. *Nat. Commun.* **9**, 4608 (2018).
3. F. Waldhauser, D. P. Schaff, T. Diehl, E. R. Engdahl, Splay faults imaged by fluid-driven aftershocks of the 2004 M-w 9.2 Sumatra-Andaman earthquake. *Geology* **40**, 243–246 (2012).
4. L. Wang, C. K. Shum, F. J. Simons, B. Tapley, C. Dai, Coseismic and postseismic deformation of the 2011 Tohoku-Oki earthquake constrained by GRACE gravimetry. *Geophys. Res. Lett.* **39**, L07301 (2012).
5. R. H. Sibson, An episode of fault-valve behaviour during compressional inversion? The 2004 M_J6.8 Mid-Niigata Prefecture, Japan, earthquake sequence. *Earth Planet. Sci. Lett.* **257**, 188–199 (2007).
6. F. Cappa, J. Rutqvist, K. Yamamoto, Modeling crustal deformation and rupture processes related to upwelling of deep CO_2-rich fluids during the 1965–1967 Matsushiro earthquake swarm in Japan. *J. Geophys. Res.* **114**, B10304 (2009).
7. K. Umeda, K. Asamori, T. Negi, T. Kusano, A large intraplate earthquake triggered by latent magmatism. *J. Geophys. Res.* **116**, B01207 (2011).
8. J. Noir, E. Jacques, S. Békri, P. M. Adler, P. Tapponnier, G. C. P. King, Fluid flow triggered migration of events in the 1989 Dobi Earthquake sequence of central Afar. *Geophys. Res. Lett.* **24**, 2335–2338 (1997).
9. S. A. Miller, C. Collettini, L. Chiaraluce, M. Cocco, M. Barchi, B. J. P. Kaus, Aftershocks driven by a high-pressure CO_2 source at depth. *Nature* **427**, 724–727 (2004).
10. T. Terakawa, A. Zoporowski, B. Galvan, S. A. Miller, High-pressure fluid at hypocentral depths in the L'Aquila region inferred from earthquake focal mechanisms. *Geology* **38**, 995–998 (2010).
11. F. Di Luccio, G. Ventura, R. Di Giovambattista, A. Piscini, F. R. Cinti, Normal faults and thrusts reactivated by deep fluids: The 6 April 2009 M-w 6.3 L'Aquila earthquake, central Italy. *J. Geophys. Res.* **115**, B06315 (2010).
12. F. Di Luccio, G. Chiodini, S. Caliro, C. Cardellini, V. Convertito, N. A. Pino, C. Tolomei, G. Ventura, Seismic signature of active intrusions in mountain chains. *Sci. Advanc.* **4**, e1701825 (2018).
13. T. Fischer, C. Matyska, J. Heinicke, Earthquake-enhanced permeability - evidence from carbon dioxide release following the M_L 3.5 earthquake in West Bohemia. *Earth Planet. Sci. Lett.* **460**, 60–67 (2017).
14. F. Girault, L. B. Adhikari, C. France-Lanord, P. Agrinier, B. P. Koirala, M. Bhattarai, S. S. Mahat, C. Groppo, F. Rolfo, L. Bollinger, F. Perrier, Persistent CO_2 emissions and hydrothermal unrest following the 2015 earthquake in Nepal. *Nat. Commun.* **9**, 2956 (2018).
15. I. Barnes, P. W. Irwin, D. E. White, Global Distribution of Carbon Dioxide Discharges, and Major Zones of Seismicity, in *Water Resources Investigation WRI 78–39* (U.S. Geological Survey, Washington, DC, 1978).
16. W. P. Irwin, I. Barnes, Tectonic relations of carbon dioxide discharges and earthquakes. *J. Geophys. Res.* **85**, 3115–3121 (1980).
17. G. Chiodini, C. Cardellini, A. Amato, E. Boschi, S. Caliro, F. Frondini, G. Ventura, Carbon dioxide Earth degassing and seismogenesis in central and southern Italy. *Geophys. Res. Lett.* **31**, L07615 (2004).
18. F. Frondini, C. Cardellini, S. Caliro, G. Beddini, A. Rosiello, G. Chiodini, Measuring and interpreting CO_2 fluxes at regional scale: The case of the Apennines, Italy. *J. Geol. Soc.* **176**, 408–416 (2019).
19. H. Lee, J. D. Muirhead, T. P. Fischer, C. J. Ebinger, S. A. Kattenhorn, Z. D. Sharp, G. Kianji, Massive and prolonged deep carbon emissions associated with continental rifting. *Nat. Geosci.* **9**, 145–149 (2016).
20. J. A. Hunt, A. Zafu, T. A. Mather, D. M. Pyle, P. H. Barry, Spatially variable CO_2 degassing in the main ethiopian rift: Implications for magma storage, volatile transport, and rift-related emissions. *Geochem. Geophys. Geosys.* **18**, 3714–3737 (2017).
21. S. Brune, S. E. Williams, R. D. Müller, Potential links between continental rifting, CO_2 degassing and climate change through time. *Nat. Geosci.* **10**, 941–946 (2017).

22. E. Guidoboni, G. Ferrari, M. D. A. Comastri, G. Tarabusi, G. Sgattoni, G. Valensise, Catalogo dei Forti Terremoti in Italia (461 a.C.-1997) e nell'area Mediterranea (760 a.C.-1500), (Istituto Nazionale di Geofisica e Vulcanologia (INGV), 2018).
23. A. Pizzi, A. Di Domenica, F. Gallovič, L. Luzi, R. Puglia, Fault segmentation as constraint to the occurrence of the main shocks of the 2016 central Italy seismic sequence. *Tectonics* **36**, 2370–2387 (2017).
24. C. Doglioni, A proposal for the kinematic modeling of W-dipping subdutions - possible application to Tyrrhenian Appennines system. *Terr. Nova* **3**, 423–434 (1991).
25. M. L. Frezzotti, A. Peccerillo, G. Panza, Carbonate metasomatism and CO_2 lithosphere-asthenosphere degassing beneath the Western Mediterranean: An integrated model arising from petrological and geophysical data. *Chem. Geol.* **262**, 108–120 (2009).
26. A. Peccerillo, M. L. Frezzotti, Magmatism, mantle evolution and geodynamics at the converging plate margins of Italy. *J. Geol. Soc. London* **171**, 407–427 (2015).
27. G. Ventura, F. R. Cinti, F. Di Luccio, N. A. Pino, Mantle wedge dynamics versus crustal seismicity in the Apennines (Italy). *Geochem. Geophys. Geosys.* **8**, Q02013 (2007).
28. C. Collettini, C. Cardellini, G. Chiodini, N. De Paola, R. E. Holddsworth, S. A. F. Smith, in *The Internal Structure of Fault Zones: Implications for Mechanical and Fluid-Flow Properties*, C. A. J. Wiberley, W. Kurz, J. Imber, R. E. Holddsworth, C. Collettini, Eds. (Geological Society, London, 2008), vol. 299, pp. 175–194.
29. G. Chiodini, A. Caliro, C. Cardellini, F. Frondini, S. Inguaggiato, F. Matteucci, Geochemical evidence for and characterization of CO_2 rich gas sources in the epicentral area of the Abruzzo 2009 earthquakes. *Earth Planet. Sci.Lett.* **304**, 389–398 (2011).
30. G. Chiodini, F. Frondini, C. Cardellini, F. Parello, L. Peruzzi, Rate of diffuse carbon dioxide Earth degassing estimated from carbon balance of regional aquifers: The case of central Apennine, Italy. *J. Geophys. Res.* **105**, 8423–8434 (2000).
31. M. Kendall, J. D. Gibbons, *Rank Correlation Method* (Oxford Univ. Press, ed. 5, New York, 1990).
32. M. D. Barberio, M. Barbieri, A. Billi, C. Doglioni, M. Petitta, Hydrogeochemical changes before and during the 2016 Amatrice-Norcia seismic sequence (central Italy). *Sci. Rep.* **7**, 11735 (2017).
33. T. Boschetti, M. Barbieri, M. D. Barberio, A. Billi, S. Franchini, M. Petitta, CO2 Inflow and Elements Desorption Prior to a Seismic Sequence, Amatrice-Norcia 2016, Italy. *Geochem. Geophys. Geosys.* **20**, 2303–2317 (2019).
34. M. Barbieri, T. Boschetti, M. D. Barberio, A. Billi, S. Franchini, P. Iacumin, E. Selmo, M. Petitta, Tracing deep fluid source contribution to groundwater in an active seismic area (central Italy): A combined geothermometric and isotopic ($\delta^{13}C$) perspective. *J. Hydrol.* **582**, 124495 (2020).
35. C. Werner, T. P. Fischer, A. Aiuppa, M. Edmonds, C. Cardellini, S. Carn, G. Chiodini, E. Cottrell, M. Burton, H. Shinohara, P. Allard, in *Deep Carbon: Past to Present*, B. N. Orcutt, I. Daniel, R. Dasgupta, Eds. (Cambridge Univ. Press, Cambridge, 2019), pp. 188–236.
36. N. De Paola, G. Chiodini, T. Hirose, C. Cardellini, S. Caliro, T. Shimamoto, The geochemical signature caused by earthquake propagation in carbonate-hosted faults. *Earth Planet. Sci. Lett.* **310**, 225–232 (2011).
37. C. D. Rowe, Å. Fagereng, J. A. Miller, B. Mapani, Signature of coseismic decarbonation in dolomitic fault rocks of the Naukluft Thrust, Namibia. *Earth Planet. Sci. Lett.* **333-334**, 200–210 (2012).
38. C. Chiarabba, S. Bagh, I. Bianchi, P. De Gori, M. Barchi, Deep structural heterogeneities and the tectonic evolution of the Abruzzi region (Central Apennines, Italy) revealed by microseismicity, seismic tomography, and teleseismic receiver functions. *Earth Planet. Sci. Lett.* **295**, 462–476 (2010).
39. G. Chiodini, C. Cardellini, S. Caliro, C. Chiarabba, F. Frondini, Advective heat transport associated with regional Earth degassing in central Apennine (Italy). *Earth Planet. Sci. Lett.* **373**, 65–74 (2013).
40. N. A. Pino, V. Convertito, R. Madariaga, Clock advance and magnitude limitation through fault interaction: The case of the 2016 central Italy earthquake sequence. *Sci. Rep.* **9**, 5005 (2019).
41. P. Baccheschi, P. De Gori, F. Villani, F. Trippetta, C. Chiarabba, The preparatory phase of the Mw 6.1 2009 L'Aquila (Italy) normal faulting earthquake traced by foreshock time-lapse tomography. *Geology* **48**, 49–55 (2019).
42. J. Précigout, C. Prigent, L. Palasse, A. Pochon, Water pumping in mantle shear zones. *Nat. Commun.* **8**, 15736 (2017).
43. L. Xue, R. Bürgmann, D. R. Shelly, C. W. Johnson, T. A. Taira, Kinematics of the 2015 San Ramon, California earthquake swarm: Implications for fault zone structure and driving mechanisms. *Earth Planet. Sci. Lett.* **489**, 135–144 (2018).
44. R. H. Sibson, Earthquake rupturing in fluid-overpressured crust: How Common? *Pure Appl. Geophys.* **171**, 2867–2885 (2014).
45. C. Chiarabba, P. De Gori, M. Cattaneo, D. Spallarossa, M. Segou, Faults geometry and the role of fluids in the 2016–2017 Central Italy seismic sequence. *Geophys. Res. Lett.* **45**, 6963–6971 (2018).
46. L. Malagnini, F. P. Lucente, P. De Gori, A. Akinci, I. Munafò, Control of pore fluid pressure diffusion on fault failure mode: Insights from the 2009 L'Aquila seismic sequence. *J. Geophys. Lett.* **117**, B05302 (2012).
47. N. D'Agostino, J. A. Jackson, F. Dramis, R. Funiciello, Interactions between mantle upwelling, drainage evolution and active normal faulting: An example from the central Appennines (Italy). *Geophys. J. Int.* **147**, 475–479 (2001).
48. D. L. Parkhurst, C. A. J. Appelo, User guide to PHREEQC (Version 2) - A computer program for speciation, batch-reaction, one-dimensional transport, and inverse geochemical calculations, *US Geological Survey, Water Resources Investigation Report, 99–4259* (U.S. Depatment of the Interior, U.S. Geological Survey, Denver, Colorado, 1999).
49. C. Boni, P. Bono, G. Capelli, Schema idrogeologico dell'Italia Centrale (Hydrogeological scheme of Central Italy). *Mem. Soc. Geol. Ital.* **35**, 991–1012 (1986).
50. M. Petitta, Hydrogeology of the middle valley of the Velino River and of the S. Vittorino Plain (Rieti, Central Italy). *Ital. J. Eng. Geol. Environ.* **1**, 157–181 (2009).
51. S. Stein, M. Wysession, *An Introduction to Seismology, Earthquakes, and Earth Structure* (Blackwell Publishing, Malden, MA, 2003).

Acknowledgments: We thank the editor G. Gaetani and three anonymous reviewers for their comments and suggestions that improved the manuscript. **Funding:** This work was supported by the MIUR, project no. PRIN2017-2017LMNLAW "Connect4Carbon." **Author contributions:** G.C. originally conceived the study and wrote the manuscript with the help of C.C., G.V., F.D.L., F.F., and J.S. G.C., C.C., F.F., and S.C. elaborated the geochemical data. F.D.L. and G.V. interpreted the seismological data. J.S. performed the statistical analyses. C.C., A.R., and G.B. performed the fieldwork. S.C. performed the isotopic analyses. All the authors reviewed the manuscript. **Competing interests:** The authors declare that they have no competing interests. **Data and materials availability:** All data needed to evaluate the conclusions in the paper are present in the paper and/or the Supplementary Materials. Additional data related to this paper may be requested from the authors.

Submitted 17 April 2020
Accepted 13 July 2020
Published 26 August 2020
10.1126/sciadv.abc2938

Citation: G. Chiodini, C. Cardellini, F. Di Luccio, J. Selva, F. Frondini, S. Caliro, A. Rosiello, G. Beddini, G. Ventura, Correlation between tectonic CO_2 Earth degassing and seismicity is revealed by a 10-year record in the Apennines, Italy. *Sci. Adv.* **6**, eabc2938 (2020).

Science Advances

Correlation between tectonic CO_2 Earth degassing and seismicity is revealed by a 10-year record in the Apennines, Italy

G. Chiodini, C. Cardellini, F. Di Luccio, J. Selva, F. Frondini, S. Caliro, A. Rosiello, G. Beddini and G. Ventura

Sci Adv **6** (35), eabc2938.
DOI: 10.1126/sciadv.abc2938